Tumor and Stem Cell Biology

Cancer Research

Chromatin Remodeling Is Required for Gene Reactivation after Decitabine-Mediated DNA Hypomethylation

Jiali Si[1,2], Yanis A. Boumber[1], Jingmin Shu[1], Taichun Qin[1], Saira Ahmed[1], Rong He[1], Jaroslav Jelinek[1], and Jean-Pierre J. Issa[1,2]

Abstract

The DNA hypomethylating drug decitabine (DAC) reactivates silenced gene expression in cancer and is approved for the treatment of the myelodysplastic syndrome. Gene reactivation after DAC is variable and incompletely understood. Here, we established a cell line system (YB5) derived from the SW48 colon cancer cell line to study DAC-induced reactivation. YB5 contains a hypermethylated cytomegalovirus promoter driving green fluorescent protein (GFP), and the locus is transcriptionally silent. GFP reexpression can be achieved by DAC treatment, but the expression level of individual cells is heterogeneous. DAC-treated YB5 cells were separated into GFP-positive and GFP-negative subpopulations. By comparing DAC-treated sorted GFP-positive and GFP-negative cells, we found that their methylation levels were similarly decreased but that histone modifications and histone H3 densities were remarkably different. Despite a similar degree of (incomplete) DNA hypomethylation, GFP-positive cells reverted to an active chromatin structure marked by higher H3K9 acetylation, lower H3K27 trimethylation, and lower promoter nucleosome density. GFP-negative cells had histone modifications and promoter nucleosome density, similar to parental cells. On DAC withdrawal, gradual resilencing and remethylation occurred in both GFP-positive and GFP-negative cells, and the resilencing correlated with a gradual increase in nucleosome occupancy in GFP-positive cells. These data show that hypomethylation alone after DAC is insufficient for gene expression induction, and that chromatin resetting to an active state including nucleosome eviction is required for activation of protein expression. Our findings suggest that gene expression is the key in optimizing DAC treatment strategies in the clinic. *Cancer Res; 70(17): 6968–77. ©2010 AACR.*

Introduction

More than 50% of all human promoters are contained in CpG islands (1), and many show aberrant hypermethylation in cancer, especially tumor suppressor genes (2, 3). Abrogation of hypermethylation and reversal of epigenetic silencing is recognized as a powerful tool in cancer therapeutics (4). The compound decitabine (5-aza-2′-deoxycytidine, or DAC) is an approved drug in the treatment of myelodysplastic syndromes (5) and is currently in clinical trials in a variety of solid tumors (6–8). However, the precise mechanisms and dynamics of gene reactivation after hypomethylation induction are not well understood. DAC inhibits DNA methyltransferase activity and passive global hypomethylation is induced when the cells divide (9). Eventually, this hypomethylation restores gene expression at silent promoters (10). The required minimum degree of hypomethylation for gene reactivation is largely unknown. DNA methylation has been associated with an altered chromatin structure, presumed to be related to recruitment of histone modifiers by DNA methylation (2, 11). This has been proposed to explain the observed synergy at the gene expression level between DAC and histone deacetylase (HDAC) inhibitors (12). It has also been suggested that gene reactivation after DAC happens despite persistent or increased binding by polycomb group proteins (13), which usually silence gene expression. Part of the difficulty in understanding the precise events after DAC exposure is the marked cell-to-cell and gene-to-gene heterogeneity in gene reactivation. This heterogeneity implies that, in most studies, mixed populations of expressing/nonexpressing cells are examined.

To overcome this problem, we developed a cell line system whereby green fluorescent protein (GFP) expression is controlled by a methylated cytomegalovirus (CMV) promoter. After sorting GFP-positive and GFP-negative cells, we observe that DAC-induced gene expression does not require full demethylation, and that induction of hypomethylation alone is not sufficient to activate gene expression. The essential determinant seems to be chromatin remodeling to an active state after hypomethylation induction. Our findings also

Authors' Affiliations: [1]Department of Leukemia, The University of Texas M.D. Anderson Cancer Center and [2]Graduate School of Biomedical Sciences, The University of Texas, Houston, Texas

Note: Supplementary data for this article are available at Cancer Research Online (http://cancerres.aacrjournals.org/).

Corresponding Author: Jean-Pierre J. Issa, Department of Leukemia, The University of Texas M.D. Anderson Cancer Center, 1515 Holcombe Boulevard, Unit 0425, Houston, TX 77030. Phone: 713-745-2260; Fax: 1-713-745-2261; E-mail: jpissa@mdanderson.org.

doi: 10.1158/0008-5472.CAN-09-4474

provide the molecular basis for the variation in gene expression induction by hypomethylation and suggest the optimal use of DAC in the clinic.

Materials and Methods

Transfection of a methylated pCMV-GFP construct and clone characterization

A patch methylated construct was modified from pEGFP-N1 (Clontech). By *in vitro* methylation (*Sss*I methylase; NEB), restriction enzyme (*Pci*I and *Bgl*II; NEB) digestion, and religation (T4 ligase; NEB), the final construct had the methylation restricted to the pCMV region (Fig. 1A). The linearized patch-methylated construct was transfected into SW48 cells using Lipofectamine 2000 (Invitrogen). After G418 (Invitrogen) selection, GFP-negative cells were selected out using a FACSAriaII (BD Biosciences) for single-cell cloning. The isolated single clones were further examined for transgene copy number using real-time PCR (Supplementary Fig. S2) and for genomic insertion site using inverse PCR (Fig. 1B).

Cell culture, drug treatment, fluorescence-activated cell sorting analysis, and cell sorting

Both SW48 cells (American Type Culture Collection) and the derived single-cell clones were cultured in IL-15 medium with 10% fetal bovine serum and 100 μg/mL streptomycin-penicillin. Daily treatment with DAC (Sigma) was adopted for GFP reactivation. GFP-positive cell percentages were measured using a BD FACSCalibur flow cytometer; GFP cell sorting was conducted using BD FACSAriaII. Post-sorting analysis was performed to assess the purity of the groups. Flow sorting and fluorescence-activated cell sorting (FACS) data were processed using FlowJo (TreeStar).

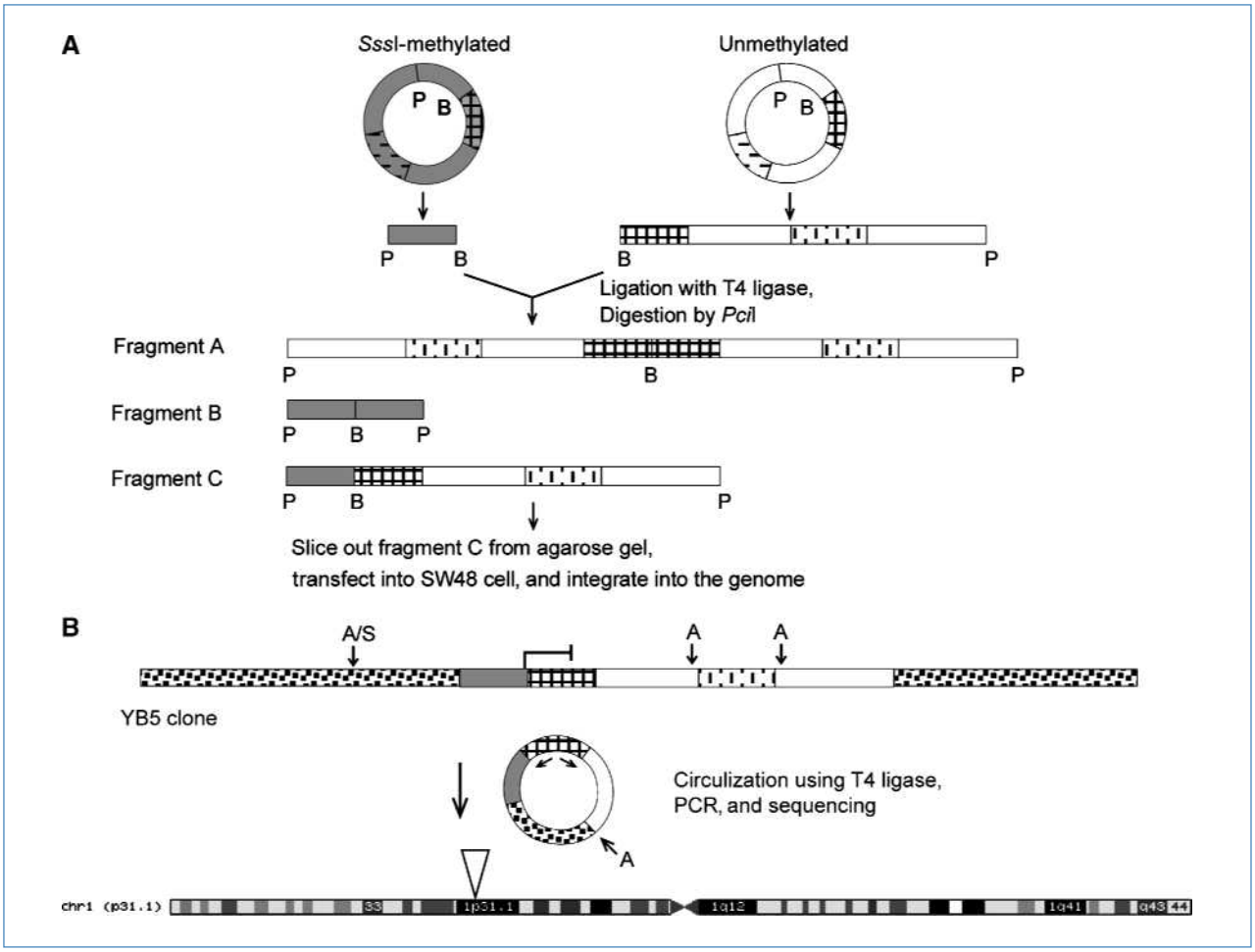

Figure 1. Generation of patch-methylated vector and establishment of YB5 single-cell clone. A, flowchart of hybrid vector construction and integration into SW48 cells. A methylated CMV fragment was inserted into the unmethylated vector backbone at *Pci*I (P) and *Bgl*II (B) sites, followed by linearization by *Pci*I digestion. Gray shade, methylated plasmid; white line, unmethylated plasmid. Gridded line, GFP element; dashed line, Neo^r element. B, in YB5 single clone, the CMV-GFP transgene locates on one allele of the chromosome 1 p31.1 region. YB5 genome was digested and a fragment containing CMV-GFP and adjacent genomic sequence was created. A, *Avr*II site; A/S, *Avr*II or *Spe*I site. Dotted rectangles represent the endogenous genomic sequence; opposing arrows point to inverse-PCR primers. The position of CMV-GFP linked genomic fragment was indicated by the triangle.

DNA extraction, bisulfite conversion, and methylation analysis

Extraction and bisulfite conversion of genomic DNA were carried out as described previously (14–16). Pyrosequencing and bisulfite cloning/sequencing were used to study methylation levels. Primers/conditions are listed in Supplementary Table S1.

RNA extraction, cDNA synthesis, quantitative real-time PCR, and 5′-rapid amplification of cDNA ends

Total RNA was extracted using Trizol (Invitrogen); the residual genomic DNA was removed using DNA-Free kit (Ambion); and cDNA was synthesized using High-Capacity cDNA Kit (Applied Biosystems). Quantification of cDNA was done by real-time PCR using ABI Prism 7900HT system. All cDNA products were amplified with the Universal PCR Master Mix (Bio-Rad) and done in triplicate. *GAPDH* was used as a reference gene. Primers/probes are listed in Supplementary Table S1. 5′ Rapid amplification of cDNA ends (5′-RACE) was done using a 5′-RACE kit (Invitrogen) to determine the transcription start site (TSS) of *GFP* gene. Total RNA from 100 nmol/L DAC–treated YB5 cells was used as template and the GFP-specific primers are listed in Supplementary Table S1.

Chromatin immunoprecipitation

Chromatin immunoprecipitation (ChIP) analyses were performed as described previously (17). Cells were 1% formaldehyde fixed and lysed followed by sonication shearing using the Biorupter (Diagenode). Antibodies used were anti–histone H3 (ab1791, Abcam), anti–histone H3K9 acetylation (07-352, Millipore), anti–histone H3K27 trimethylation (07-449, Millipore), and anti-IgG (ab46540, Abcam). The value of each histone mark was determined by H3 and IgG normalization using the following equation: enrichment = $2^{[Ct(H3) - Ct(Ab)]} - 2^{[Ct(H3) - Ct(IgG)]}$. The value of histone H3 protein enrichment was determined by input control. One percent of chromatin was used as input control. Quantification of ChIP DNA was done by real-time PCR, and primers/probes are listed in Supplementary Table S1.

Histone preparation and Western blots

Total histones were prepared by acidic extraction and resolved on 15% SDS-polyacrylamide gels as described (18). Additional antibodies used were anti–pan-acetylated histone H4 (06-866, Millipore) and anti–histone H4 (07-108, Millipore).

Results

An integrated and silenced CMV-GFP transgene

We started deriving a DNA methylation reporter assay by transfecting an *in vitro* methylated CMV-GFP transgene into the colon cancer cell line SW48, which has intense hypermethylation of multiple genes characteristic of the CIMP subtype of colon cancers (19). CMV promoter is >500 bp in length and includes 30 CpG sites with a CpG percentage of 6%; the ObsCpG/ExpCpG ratio is 0.89 and the GC content is 50%. Thus, the CMV promoter is a classic CpG island following Gardiner-Garden and Frommer's criteria. The outline of generating a patch-hypermethylated plasmid and transfection into SW48 is presented in Fig. 1A. After selection, sorting, and single-cell cloning, we tested multiple isolates for the required characteristics (integrated intact transgene, silenced gene expression) and characterized one, YB5, in detail. We used quantitative PCR to determine that the transgene dosage in YB5 genome was one (Supplementary Fig. S2). Copy number did not change over a time period of up to 15 months (data not shown). We next used inverse PCR to determine the integration site. The resulting PCR product contained a 774-bp-long sequence with 100% homology to position 73061660–73062433 of the minus strand on chromosome 1 in the UCSC BLAT database (hg18, March 2006; Fig. 1B). Thus, the transgene integrated into an intragenic region of human EST CD655906 on chromosome 1p31.1. We also used a GFP-expressing clone, YB11, which contained one copy of CMV-GFP transgene at chromosome 19p13.3 region as a positive control for subsequent experiments.

DNA methylation controls silencing of the transgene

We used quantitative bisulfite pyrosequencing and bisulfite cloning/sequencing to study the DNA methylation state of the transgene in detail. Bisulfite pyrosequencing revealed that the CMV promoter in the GFP-expressing clone YB11 was unmethylated, whereas the silenced clone YB5 was hypermethylated from −337 to +19 bp of the transcription start site (Fig. 2A). This region covers the core CMV promoter and contains 22 CpG sites with an average methylation level >80%. Analysis of early and late cell passages of YB5 showed that the methylation pattern is stable. The hypermethylation pattern was also confirmed by bisulfite cloning/sequencing using another set of PCR primers (Fig. 2B). Almost every CpG site had very high levels of DNA methylation, with the exception of two CpG sites that correspond to cAMP-responsive element binding protein (CREB) binding sites indicated by Genomatix Software analysis. Interestingly, we detected no binding of CREB or phospho-CREB to the region in the YB5 cells, whereas binding was detected in YB11 by ChIP assays (Supplementary Fig. S3).

Next, we investigated the effect of CMV hypermethylation on the expression of the *GFP* gene. Using quantitative real-time PCR, we found robust GFP expression in YB11 and no GFP mRNA in YB5 and SW48. Using the hypomethylating agent DAC at different concentrations (from 10 to 200 nmol/L), the YB5 *GFP* gene could be reactivated in a dose-dependent manner (Fig. 3A). Because DAC can have effects independent of DNA methylation (20), we also tested whether gene reactivation can be achieved by directly inhibiting DNMT1, the main DNA methyltransferase. Using DNMT1 siRNA knockdown (21), we found efficient GFP reactivation compared with the scrambled control. By contrast, knockdown of EZH2 had no effect on GFP reactivation (Supplementary Fig. S4). Furthermore, to determine whether the DAC-reactivated GFP transcript is driven by the CMV promoter, a 5′RACE experiment was conducted, which confirmed that the GFP mRNA starts from the 3′end of the CMV promoter. Thus, the integrated transgene is silenced

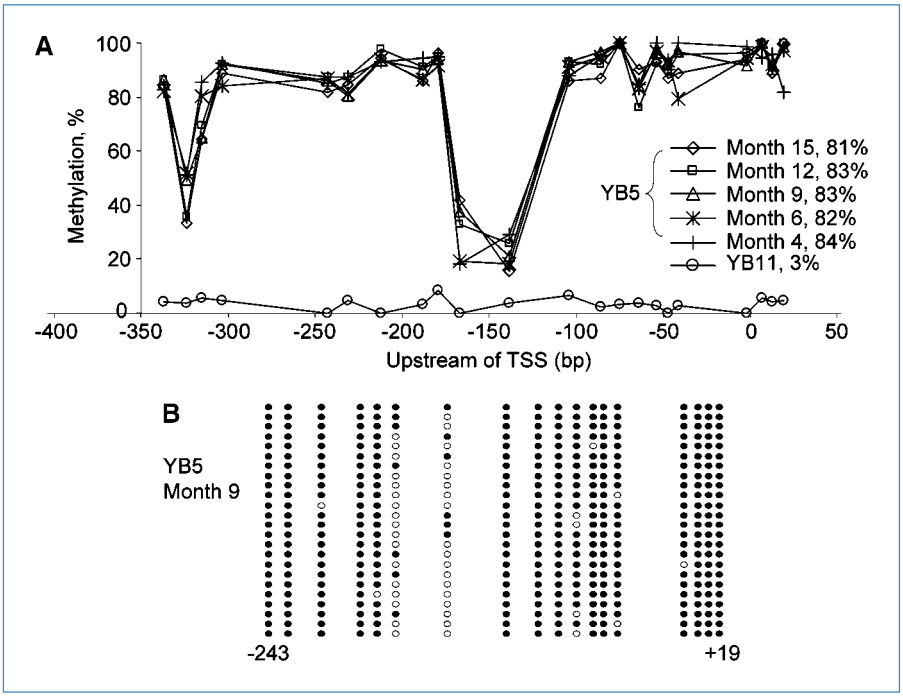

Figure 2. The CMV promoter is hypermethylated in YB5. A, pyrosequencing results of 22 individual CpG sites of the promoter region. The location of each CpG site relative to the transcription start site is shown on the *X* axis and the percentages of methylated cytosines at each CpG site are dot-plotted on the *Y* axis. Five different passages of YB5 cells were analyzed and the overall methylation averaged from 22 CpG sites was indicated. By contrast, the GFP-expressing YB11 clone is unmethylated. B, bisulfite cloning/sequencing analysis of YB5 cells at month 9. Filled and open circles represent methylated and unmethylated CpGs, respectively. Each strand of circles represents one allele obtained from one bacterial clone, and circles were placed relative to scale.

by DNA methylation and mimics endogenous tumor suppressor gene silencing in cancer.

Heterogeneous GFP reactivation after DAC

We next used FACS flow cytometry to analyze GFP reactivation. As can been seen in Fig. 3B, SW48 and YB5 cells stayed at the GFP-negative region and YB11 fell into the GFP-positive region, whereas the 100 nmol/L DAC–treated YB5 cells exhibited a distribution shift to the GFP-positive region. The percentages of GFP-positive cells under the gradient DAC treatment are summarized in Fig. 3C. The correlation of GFP percentages from FACS analysis with mRNA expression levels determined by quantitative real-time PCR was analyzed and found an R^2 value of 0.97 (Fig. 3D). Taking advantage of the single-cell detection of GFP expression enabled by flow analysis, we observed a large difference in expression levels of individual cells originating from an identical cell population after a demethylating stimulus. Moreover, the proportion of cells positive for GFP did not exceed 40%, even with increasing doses or duration of exposure. Previous studies analyzed DAC-treated cells as a uniform population, whereas the single-cell analysis captures this very heterogeneous behavior.

Hypomethylation is not sufficient to activate GFP expression

To explore the mechanisms underlying heterogeneity in gene expression after DAC treatment, we separated GFP-positive and GFP-negative subpopulations using a cell sorting cytometer (Fig. 4A). Post-sorting analysis revealed that the purity of sorted populations was about 85% in the GFP-positive subpopulation and 98% in the GFP-negative subpopulation. The sorted cells were collected and methylation levels were studied. The first question we asked is whether the difference in gene expression is simply due to lack of hypomethylation in a subpopulation of cells, perhaps related to quiescence at the time of exposure. The CMV promoter methylation was first investigated using pyrosequencing and found that the GFP-positive cells demethylated from 81.4 ± 0.2% to 45.4 ± 0.2% and the GFP-negative cells to 51.1 ± 0.1% (Fig. 4B). We next used bisulfite cloning/sequencing on these cells and found that DNA methylation is mosaic and overall similar between positive and negative cells (Fig. 4C). Besides the CMV promoter, we also examined global methylation status using the long interspersed nucleotide element-1 (LINE1) repetitive element (22, 23), and we found that global methylation decreased from 58.0 ± 0.3% to 39.0 ± 0.4% in GFP-positive cells and to 41.9 ± 0.1% in GFP-negative cells. Similarly, we found no differences in methylation levels of genes *P16^{INK4a}*, *CDH13, RASSF1a, RARβ2*, and *PGRB* between sorted subpopulations (Fig. 4D, left). The expressions of *P16^{INK4a}*, *RASSF1a*, and *PGRB* were measured, and P16^{INK4a} and RASSF1a were reactivated by DAC whereas PGRB was not. Similar to GFP, the expressions of P16^{INK4a} and RASSF1a were higher in GFP-positive cells than in GFP-negative cells (Fig. 4D, right). These data suggest that a decrease in methylation may be necessary but is not sufficient for gene reactivation after DAC; other critical events must be involved. Cell cycle distributions of GFP-positive and GFP-negative cells were analyzed, but no differences were found (data not shown).

To ensure that our results are not strictly due to the presence of hemimethylated DNA, we repeated the experiment with a one-time DAC treatment, and we still saw partial

methylation associated with transcription and a relatively small difference between GFP-positive and GFP-negative cells (Supplementary Fig. S5).

Chromatin reprogramming is required for activated GFP expression

Because chromatin structure is also critical to regulate silencing and gene expression in mammalian cells, we examined histone modifications in parental cells and DAC-treated GFP-positive/GFP-negative subpopulations. Several modification marks were investigated using ChIP assays, including histone H3 lysine 9 acetylation (H3K9ac), lysine 4 trimethylation (H3K4me3), lysine 9 trimethylation (H3K9me3), and lysine 27 trimethylation (H3K27me3). Three regions along the CMV-GFP locus were studied, including the promoter region (–200 bp), TSS region, and GFP coding region (+400 bp).

The parental YB5 cells exhibited a closed chromatin structure, devoid of H3K9ac and enriched for H3K27me3, whereas the expressing YB11 cells were just the opposite. After DAC, the hypomethylated GFP-negative cells were similar to parental cells, retaining low H3K9ac and high H3K27me3 levels, whereas the GFP-positive cells showed chromatin reverting to an active state, with 2.5- to 5-fold higher level of H3K9ac and 2.5- to 8-fold lower level of H3K27me3 compared with the GFP-negative cells. Although histone H3K4me3 and H3K9me3 were different between YB5 and YB11 cells, they were not found to be distinguishable in GFP-positive and GFP-negative cells. Also, the ChIP assay did not show binding of CREB in either GFP-positive or GFP-negative cells (data not shown). Interestingly, histone H3 densities at the promoter and TSS regions were found to be very different between GFP-positive and GFP-negative cells. The GFP-positive cells showed H3 loss, suggesting promoter nucleosome eviction, whereas the GFP-negative cells retained most of the histone H3 of the parental YB5 cells (Fig. 5A). By contrast, we performed Western blot analysis and found no differences in global histone marks between the GFP-positive and GFP-negative cell populations (Fig. 5B).

To verify that the active chromatin state could occur despite residual DNA methylation, we performed bisulfite pyrosequencing on DNA immunoprecipitated with histone H3K9ac and histone H3K27me3 antibodies. We found that

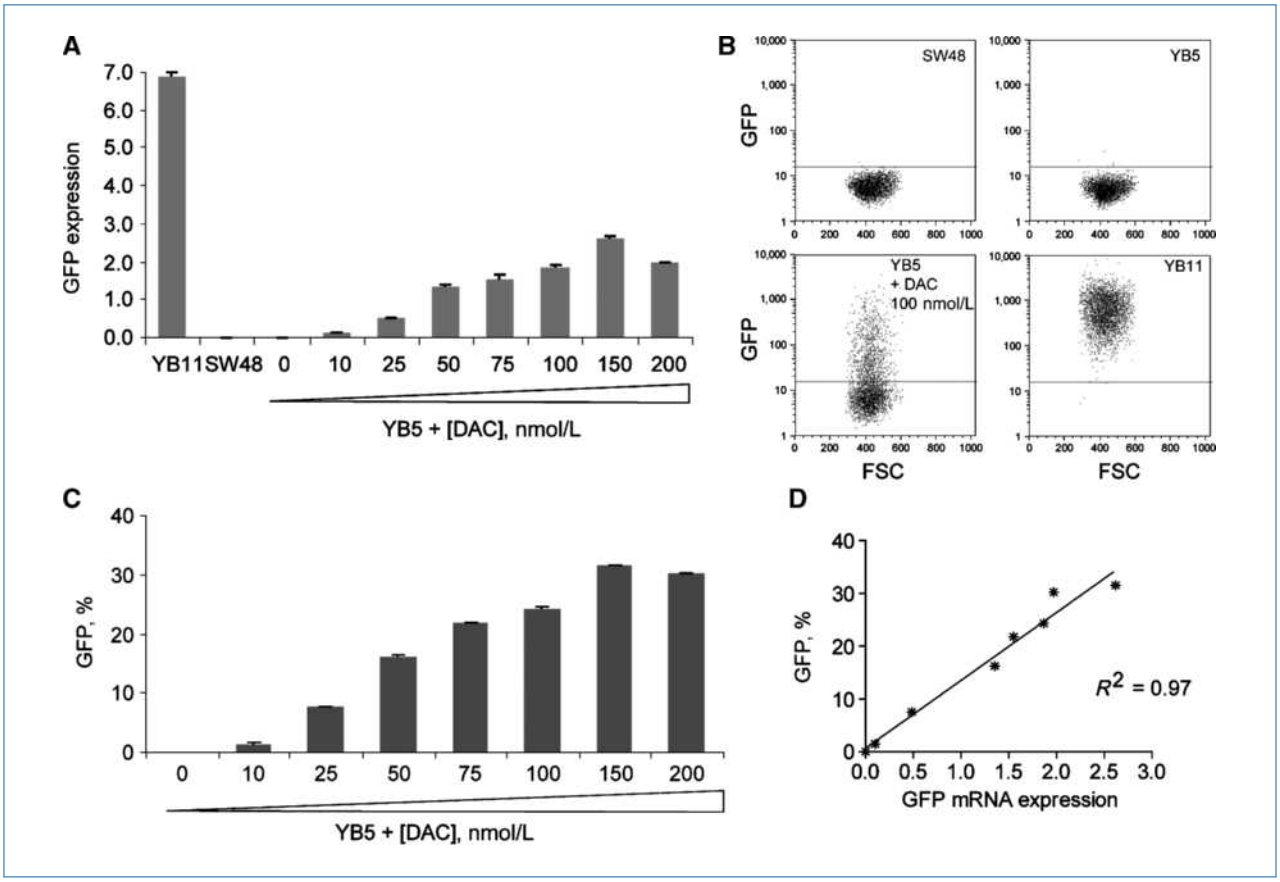

Figure 3. GFP is silenced in YB5 and heterogeneously reactivated by DAC. A, expression of GFP mRNA in SW48, YB5, and gradient DAC–treated YB5 cells. Four days of treatment of gradient amount of DAC restored GFP expression in a dose-dependent manner. YB11 clone, positive control. B, fluorescent plots of SW48, YB5, YB11, and DAC-reactivated YB5 cells (100 nmol/L treatment as an example). C, FACS analysis of GFP positivity of YB5 cells treated with increasing amounts of DAC described in A. The cutoff line of GFP positivity is shown as the horizontal line in B. D, correlation of percent GFP obtained by FACS analysis to mRNA expression obtained by real-time PCR. The correlation was significant ($P < 0.05$) as determined by Pearson test.

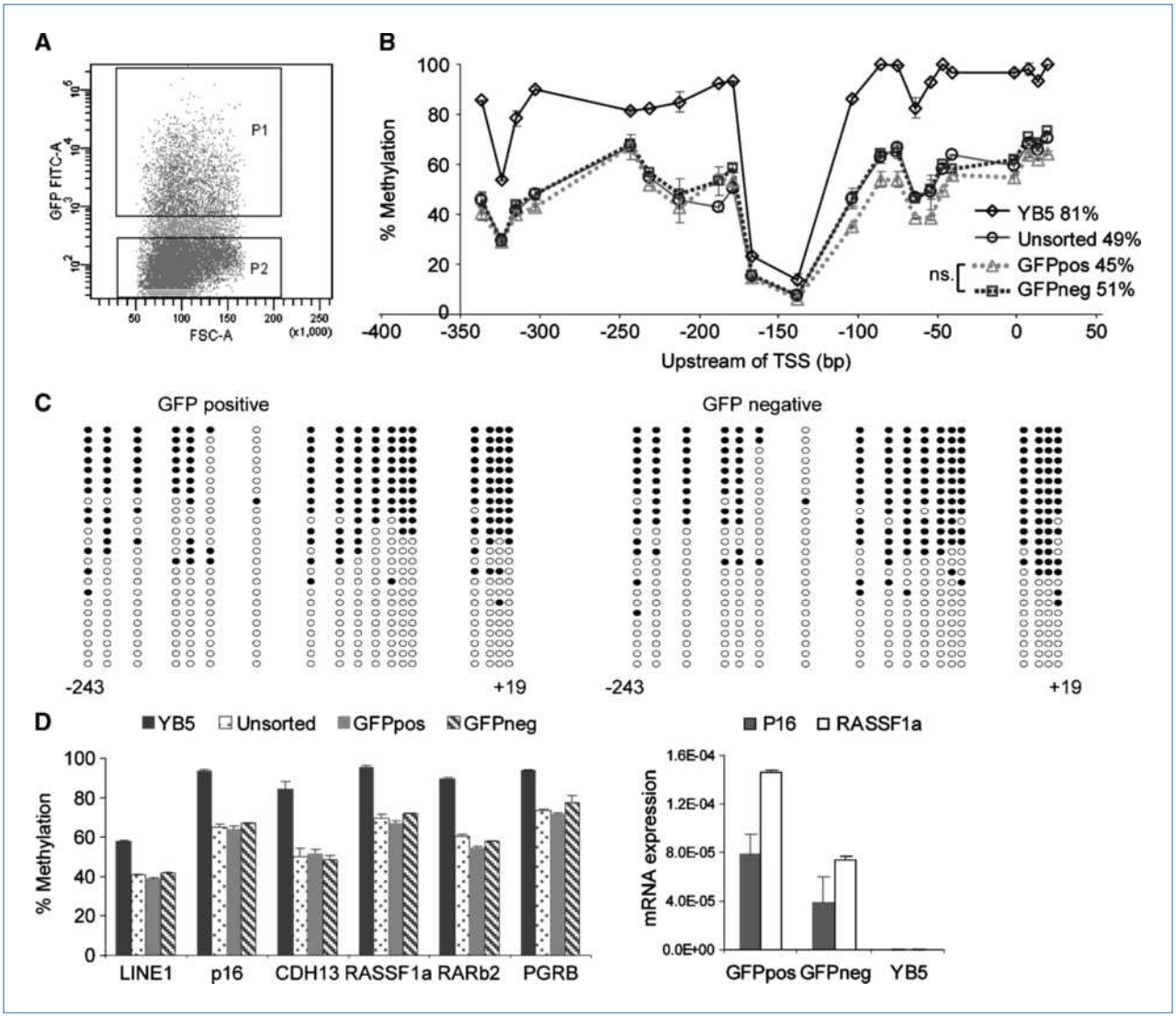

Figure 4. Hypomethylation is not sufficient to activate GFP expression. A, YB5 cells were treated with 100 nmol/L DAC for 96 h, and then sorted into GFP-positive (P1) and GFP-negative (P2) subpopulations. B, CMV promoter methylation levels on day 0 after sorting in non–DAC-treated, DAC-treated, and sorted subgroups, measured by pyrosequencing. C, bisulfite cloning/sequencing analysis of CMV promoter on GFP-positive and GFP-negative subgroups at day 0 after sorting. D, left, global methylation level (LINE1) and methylation levels of individual genes, measured by pyrosequencing; right, gene expressions in sorted subgroups. Bars, SD. ns, no statistical significance.

H3K9ac-bound DNA is 31% methylated, H3K9ac-unbound DNA is 56% methylated, H3K27me3-bound DNA is 59% methylated, and H3K27me3-unbound DNA is 54% methylated. The methylation level is the average of seven CpG sites located from −104 to −41 bp from the TSS. These data show that at the CMV promoter locus, H3K9-acetylated histones can be present on methylated DNA, but shows a preference to less methylated DNA; H3K27-trimethylated histones have no particular DNA methylation preference (Supplementary Fig. S6).

HDAC inhibitors can increase global histone acetylation; we therefore asked if altering histone marks by treatment with the HDAC inhibitor TSA would promote the expression of the sorted GFP-negative cells. Low doses of TSA showed no effect on the fully methylated YB5 cells. As shown in Fig. 5C, 24 hours after sorting, the hypomethylated but initially GFP-negative cells had about 12% GFP-positive cells, likely representing the continuing effects of DAC. TSA treatment increased this number to 46%, which indicated that the synergy was achieved at the GFP locus. As expected, in GFP-positive cells, TSA had little effect on boosting gene expression further. Using ChIP assays, we confirmed that TSA treatment elevated histone H3K9ac at the CMV locus but decreased histone H3K27me3. However, the post-TSA treatment did not affect histone H3 density in GFP-negative cells (data not shown).

GFP expression has no effect on DNA remethylation

After DAC-induced hypomethylation, gene remethylation is the norm (24, 25), although the mechanisms of this phenomenon are unknown. It has been proposed that a residual closed chromatin state predisposes to remethylation and that high levels of gene expression may protect against remethylation (26). This important question could be addressed using this model. To do this, we cultured the sorted cells separately and followed DNA methylation over time. The percentage of GFP-positive cells over a 48-day period is shown in Fig. 6A and the methylation at each time point is shown in Fig. 6B. As can be seen, after DAC withdrawal, GFP-positive cells decreased in a two-phase fashion: a rapid reduction at the first several days (up to day 5) and a slow decrease later on. Remethylation occurs in both populations, and the rate of remethylation is identical in sorted GFP-positive and GFP-negative cells. We also tested the effect of prolonged TSA treatment, but it did not prevent remethylation of either GFP-positive cells or GFP-negative cells (data not shown).

Because gene expression seems to decline more rapidly than DNA remethylation, we examined chromatin changes focusing on the nucleosome occupancy of promoter and TSS regions. Histone H3 densities of GFP-positive and GFP-negative cells at day 2 and day 5 were examined. Combining the day 0 data from Fig. 5A, the nucleosome recovery kinetics is shown in Fig. 6C. We found that an increase in histone H3 occurred rapidly after DAC withdrawal, and the speed of GFP-positive cells was faster than that of GFP-negative cells. This nucleosome reassembly in GFP-positive cells seems to be correlated with the rapid phase of GFP resilencing. Collectively, the DAC-induced chromatin remodeling is short lived. The rate of DNA remethylation was not dependent on the expression levels or chromatin structure after DAC and thus may relate to the residual DNA methylation marks near the CMV-GFP locus.

Discussion

In this study, we describe a new model system YB5, which contains a hypermethylated and silenced CMV-driven *GFP* gene, with stably inherited epigenetic properties established over time. In this model, the promoter is DNA hypermethylated

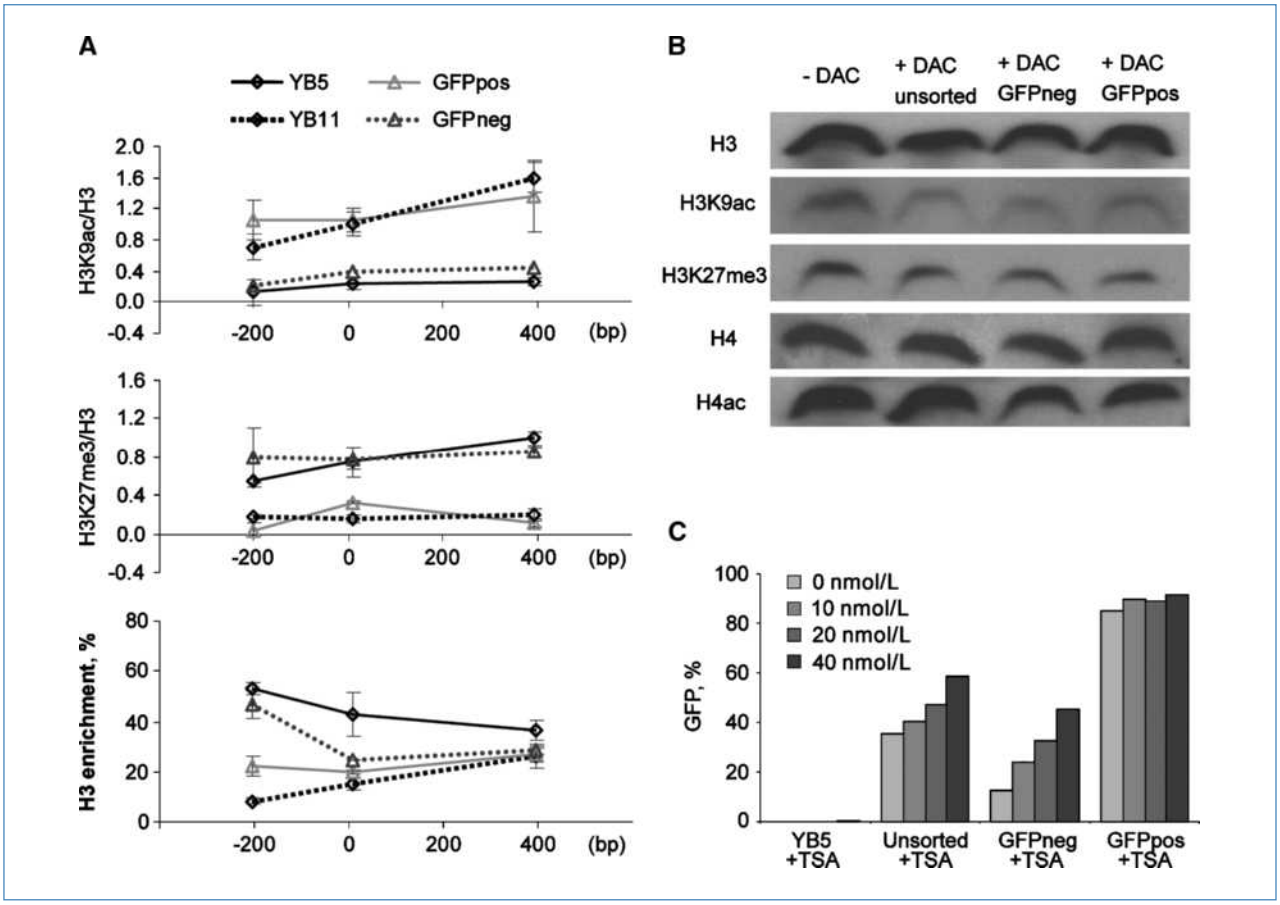

Figure 5. Chromatin reprogramming is required for activated GFP expression. A, ChIP-quantitative PCR for the enrichments of H3K9ac, H3K27me3, and H3 on DAC-treated sorted GFP-positive and GFP-negative cells on day 0 after sorting. Each value is the average result from two or three independent ChIP experiments. Positions studied are indicated on the *X* axis; bars, SD. B, Western blot analysis for modified and total histone protein levels in sorted subgroups on day 0 after sorting. C, percent GFP of sorted cell subgroups 24 h after TSA treatment with the indicated doses. Columns, GFP-positive cell percentage.

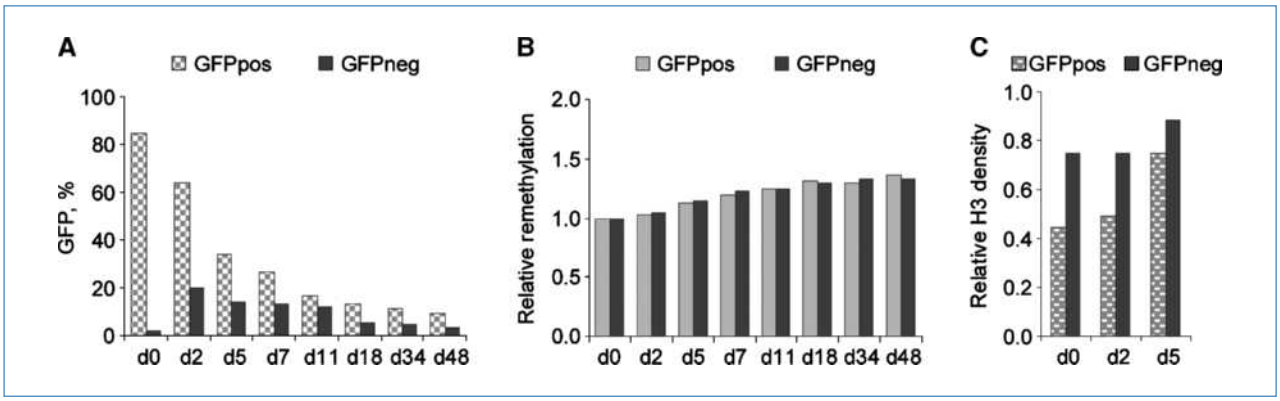

Figure 6. GFP resilencing, DNA remethylation, and histone recovery. A, resilencing kinetics of GFP in sorted GFP-positive and GFP-negative subpopulations over 48 d after sorting. *Y* axis, % of GFP-positive cells; *X* axis, days after sorting. B, remethylation kinetics of CMV promoter in GFP-positive and GFP-negative cells. The methylation value of each time point was the average of 22 CpG sites and normalized to the methylation value of day 0 after sorting. *Y* axis, relative remethylation level. C, histone H3 recovery kinetics. The relative density was the sum value of promoter and TSS regions normalized with that of YB5. Day 2 and day 5 samples were ChIP-quantitative PCR analyzed (day 0 and YB5 data from Fig. 5A combined). *Y* axis, relative H3 level.

and has a closed chromatin structure characterized by histone H3K9 deacetylation and H3K27 hypermethylation. Expression is suppressed at the transcriptional level and can be restored by using the demethylating agent DAC or by inhibiting DNMT1 expression. Thus, this system mimics many of the features of typical gene silencing in mammalian cells, including cancer cells. CMV is a strong CpG island–containing promoter, and it can be efficiently silenced as previously reported (27, 28). Because reactivated gene expression can be easily visualized and selected for, this model allowed us to ask important questions about the minimal requirements for gene reactivation, as well as to track resilencing after epigenetic modulation. These questions have previously been investigated primarily from the perspective of entire (mixed) cell populations, although one study used subcloning and gene expression selection to ask questions about remethylation (9).

We first asked about the association between hypomethylation induction and gene reactivation. Surprisingly, methylation studies showed similar demethylation levels between GFP-positive and GFP-negative cells, which suggests that pharmacologic uptake of DAC is uniform and not rate-limiting in these cells. In sorted cells that had high GFP expression, DNA methylation did not decrease to normal levels (nearly zero), suggesting that a previous hypothesis about heterogeneous reexpression being explained by a mixture of cells demethylated to 0% (and reexpressing) while others remain hypermethylated and silenced is incorrect. In fact, only 6 of 24 alleles sequenced had complete demethylation in these cells with high GFP expression. Thus, only a moderate degree of DNA hypomethylation is required for gene reactivation. In our experiments, we ruled out activation of an alternative host promoter as a possible explanation. However, further experiments may be needed to verify that methylated CpG islands can still have promoter activity if they retain an open chromatin. Bisulfite sequencing analysis of H3K9ac histones showed about 30% DNA methylation, confirming that the gene can be activated despite residual DNA methylation, but also suggesting that unmethylated alleles are enriched in open chromatin. Moreover, in our data, the GFP-negative cells after DAC also had decreased DNA methylation levels, showing that DNA hypomethylation per se is not sufficient for gene reactivation. Rather, the main molecular difference between GFP-positive and GFP-negative cells after DAC was the differential histone modifications and histone H3 densities revealed by ChIP assays. Thus, chromatin resetting is the prime factor determining gene reexpression state after DAC-induced DNA demethylation. Interestingly, it has previously been reported that DAC induces nuclease sensitivity changes in the human HPRT gene locus before gene reexpression (29) and decreased nucleosome occupancy of hMLH1 promoter after DAC (30), which are consistent with our data.

It is interesting to ask why a relatively small degree of DNA demethylation would naturally, but not uniformly, bring histone changes and chromatin resetting. A possible explanation is that in the absence of DNMTs, the coupled assembly of newly synthesized histone octamers during cellular replication may be disrupted. The nascent histone octamers lose some original repressive histone tail marks, the promoter nucleosome assembly is disabled, and the chromatin alters to a locally open structure, resulting in transcription of this strand of DNA (31, 32). Indeed, DNMT1 and DNMT3b have been reported to bind to HDACs, histone methyltransferases, and chromatin scaffold proteins, and it is possible that this binding is important to replication of histone marks. It is interesting to note that after withdrawal of DAC, about 12% of sorted GFP-negative cells transform to expressing cells after 24 hours in regular growth medium, which indicates the continuing chromatin resetting. This model also explains the observed synergistic effect between DNA demethylating agents and low-dose HDAC inhibitors (12).

The cell sorting strategy also allowed us to address the vexing problem of gene resilencing and remethylation after DAC withdrawal. Using a mixed cell population, it was previously

reported that the repressive histone mark H3K27me3 persists or increases after DAC treatment (13) and thus serves as a nidus for resilencing. Our data using purified cells are not consistent with these observations. Rather, we find that resilencing and remethylation are independent of gene expression levels or of local chromatin structure. The kinetics of DNA remethylation is quite flat, which can be cell division related (33). However, loss of expression after DAC withdrawal is very rapid in the first several days (seen at day 2 and day 5). Notably, the speed of histone H3 gains up to day 5 is also prompt, which seems to be coincident with rapid GFP loss. Thus, it is highly likely that the first resilencing is due to the reassembly of nucleosomes, although the driving force of repackaging DNA is unknown. It is possible that a closed chromatin configuration persists in *cis* away from the CMV promoter and underlies gene resilencing.

It remains to be seen how much the data we have generated with this *in vitro* system are applicable to endogenous gene silencing. All indications are that they would be—the transgene is stably integrated, shows the typical methylation-associated closed chromatin configuration, and is reactivated by DAC or DNMT1 knockdown with similar kinetics and patterns as endogenous genes. Nevertheless, it is likely that there will be gene- or locus-specific events that influence reactivation Indeed, some genes are silenced without detectable H3K27me3 (33), and those may behave differently. Similarly, promoters vary in their CpG density and degree of DNA methylation, and this could influence gene reactivation patterns.

Our data have clinical implications for the use of DNA methylation inhibitors. In treated patients, relatively small decreases in DNA methylation were observed (34, 35), but these were accompanied by significant gene reactivation and clinical responses. Moreover, as would be predicted from the current data, gene reactivation was a better predictor of response than hypomethylation induction (36, 37). In a similar manner to the *in vitro* situation, gene remethylation was observed, and a higher extent of remethylation was associated with resistance to therapy (35).

In summary, we found that DNA hypomethylation is necessary but not sufficient for gene reactivation after DAC. Rather, local chromatin structure resetting, which can happen at a low level of DNA demethylation, is a key determinant of actual gene reexpression. These data have implications for the use of hypomethylating drugs in the clinic. In addition, the YB5 system can be useful for evaluating potential demethylating compounds and epigenetic synergy studies to boost gene reactivation as well as prevent resilencing and remethylation.

Disclosure of Potential Conflicts of Interest

No potential conflicts of interest were disclosed.

Grant Support

NIH grants CA100632, CA098006, and CA121104. J-P.J. Issa is an American Cancer Society Clinical Research professor supported by a generous gift from the F.M. Kirby Foundation. DNA sequencing and flow cytometry in the respective cores at the M.D. Anderson Cancer Center is supported by Core Grant CA16672 from the NIH.

The costs of publication of this article were defrayed in part by the payment of page charges. This article must therefore be hereby marked *advertisement* in accordance with 18 U.S.C. Section 1734 solely to indicate this fact.

Received 12/09/2009; revised 06/29/2010; accepted 06/30/2010; published OnlineFirst 08/16/2010.

References

1. Bird AP. CpG-rich islands and the function of DNA methylation. Nature 1986;321:209–13.
2. Jones PA, Baylin SB. The epigenomics of cancer. Cell 2007;128:683–92.
3. Nguyen CT, Gonzales FA, Jones PA. Altered chromatin structure associated with methylation-induced gene silencing in cancer cells: correlation of accessibility, methylation, MeCP2 binding and acetylation. Nucleic Acids Res 2001;29:4598–606.
4. Issa JP, Kantarjian HM. Targeting DNA methylation. Clin Cancer Res 2009;15:3938–46.
5. Kantarjian H, O'Brien S, Cortes J, et al. Therapeutic advances in leukemia and myelodysplastic syndrome over the past 40 years. Cancer 2008;113:1933–52.
6. Schrump DS, Fischette MR, Nguyen DM, et al. Phase I study of decitabine-mediated gene expression in patients with cancers involving the lungs, esophagus, or pleura. Clin Cancer Res 2006;12:5777–85.
7. Appleton K, Mackay HJ, Judson I, et al. Phase I and pharmacodynamic trial of the DNA methyltransferase inhibitor decitabine and carboplatin in solid tumors. J Clin Oncol 2007;25:4603–9.
8. Stewart DJ, Issa JP, Kurzrock R, et al. Decitabine effect on tumor global DNA methylation and other parameters in a phase I trial in refractory solid tumors and lymphomas. Clin Cancer Res 2009;15:3881–8.
9. Bender CM, Pao MM, Jones PA. Inhibition of DNA methylation by 5-aza-2′-deoxycytidine suppresses the growth of human tumor cell lines. Cancer Res 1998;58:95–101.
10. Baylin SB. DNA methylation and gene silencing in cancer. Nat Clin Pract Oncol 2005;2 Suppl 1:S4–11.
11. Fuks F, Burgers WA, Brehm A, Hughes-Davies L, Kouzarides T. DNA methyltransferase Dnmt1 associates with histone deacetylase activity. Nat Genet 2000;24:88–91.
12. Cameron EE, Bachman KE, Myohanen S, Herman JG, Baylin SB. Synergy of demethylation and histone deacetylase inhibition in the re-expression of genes silenced in cancer. Nat Genet 1999;21:103–7.
13. McGarvey KM, Van Neste L, Cope L, et al. Defining a chromatin pattern that characterizes DNA-hypermethylated genes in colon cancer cells. Cancer Res 2008;68:5753–9.
14. Shu J, Jelinek J, Chang H, et al. Silencing of bidirectional promoters by DNA methylation in tumorigenesis. Cancer Res 2006;66:5077–84.
15. Colella S, Shen L, Baggerly KA, Issa JP, Krahe R. Sensitive and quantitative universal Pyrosequencing methylation analysis of CpG sites. Biotechniques 2003;35:146–50.
16. Kroeger H, Jelinek J, Estecio MR, et al. Aberrant CpG island methylation in acute myeloid leukemia is accentuated at relapse. Blood 2008;112:1366–73.
17. Kondo Y, Shen L, Yan PS, Huang TH, Issa JP. Chromatin immunoprecipitation microarrays for identification of genes silenced by histone H3 lysine 9 methylation. Proc Natl Acad Sci U S A 2004;101:7398–403.
18. Johnson AB, Denko N, Barton MC. Hypoxia induces a novel signature of chromatin modifications and global repression of transcription. Mutat Res 2008;640:174–9.

19. Issa JP, Shen L, Toyota M. CIMP, at last. Gastroenterology 2005; 129:1121–4.
20. Missiaglia E, Donadelli M, Palmieri M, Crnogorac-Jurcevic T, Scarpa A, Lemoine NR. Growth delay of human pancreatic cancer cells by methylase inhibitor 5-aza-2′-deoxycytidine treatment is associated with activation of the interferon signalling pathway. Oncogene 2005; 24:199–211.
21. James SR, Link PA, Karpf AR. Epigenetic regulation of X-linked cancer/germline antigen genes by DNMT1 and DNMT3b. Oncogene 2006;25:6975–85.
22. Yang AS, Estecio MR, Doshi K, Kondo Y, Tajara EH, Issa JP. A simple method for estimating global DNA methylation using bisulfite PCR of repetitive DNA elements. Nucleic Acids Res 2004; 32:e38.
23. Aparicio A, North B, Barske L, et al. LINE-1 methylation in plasma DNA as a biomarker of activity of DNA methylation inhibitors in patients with solid tumors. Epigenetics 2009;4:176–84.
24. Bender CM, Gonzalgo ML, Gonzales FA, Nguyen CT, Robertson KD, Jones PA. Roles of cell division and gene transcription in the methylation of CpG islands. Mol Cell Biol 1999;19:6690–8.
25. Egger G, Aparicio AM, Escobar SG, Jones PA. Inhibition of histone deacetylation does not block resilencing of p16 after 5-aza-2′-deoxycytidine treatment. Cancer Res 2007;67:346–53.
26. McGarvey KM, Fahrner JA, Greene E, Martens J, Jenuwein T, Baylin SB. Silenced tumor suppressor genes reactivated by DNA demethylation do not return to a fully euchromatic chromatin state. Cancer Res 2006;66:3541–9.
27. Brooks AR, Harkins RN, Wang P, Qian HS, Liu P, Rubanyi GM. Transcriptional silencing is associated with extensive methylation of the CMV promoter following adenoviral gene delivery to muscle. J Gene Med 2004;6:395–404.
28. Meilinger D, Fellinger K, Bultmann S, et al. Np95 interacts with *de novo* DNA methyltransferases, Dnmt3a and Dnmt3b, and mediates epigenetic silencing of the viral CMV promoter in embryonic stem cells. EMBO Rep 2009.
29. Litt MD, Hansen RS, Hornstra IK, Gartler SM, Yang TP. 5-Azadeoxycytidine-induced chromatin remodeling of the inactive X-linked HPRT gene promoter occurs prior to transcription factor binding and gene reactivation. J Biol Chem 1997;272:14921–6.
30. Lin JC, Jeong S, Liang G, et al. Role of nucleosomal occupancy in the epigenetic silencing of the MLH1 CpG island. Cancer Cell 2007; 12:432–44.
31. Martin C, Zhang Y. Mechanisms of epigenetic inheritance. Curr Opin Cell Biol 2007;19:266–72.
32. Corpet A, Almouzni G. Making copies of chromatin: the challenge of nucleosomal organization and epigenetic information. Trends Cell Biol 2009;19:29–41.
33. Kondo Y, Shen L, Cheng AS, et al. Gene silencing in cancer by histone H3 lysine 27 trimethylation independent of promoter DNA methylation. Nat Genet 2008;40:741–50.
34. Yang AS, Doshi KD, Choi SW, et al. DNA methylation changes after 5-aza-2′-deoxycytidine therapy in patients with leukemia. Cancer Res 2006;66:5495–503.
35. Oki Y, Jelinek J, Shen L, Kantarjian HM, Issa JP. Induction of hypomethylation and molecular response after decitabine therapy in patients with chronic myelomonocytic leukemia. Blood 2008;111: 2382–4.
36. Blum W, Klisovic RB, Hackanson B, et al. Phase I study of decitabine alone or in combination with valproic acid in acute myeloid leukemia. J Clin Oncol 2007;25:3884–91.
37. Kantarjian H, Oki Y, Garcia-Manero G, et al. Results of a randomized study of 3 schedules of low-dose decitabine in higher-risk myelodysplastic syndrome and chronic myelomonocytic leukemia. Blood 2007;109:52–7.